Bioorganic & Medicinal Chemistry 18 (2010) 4516–4523

Contents lists available at ScienceDirect

Bioorganic & Medicinal Chemistry

journal homepage: www.elsevier.com/locate/bmc

Design, synthesis and biological evaluation of *trans* 2-(thiophen-2-yl)vinyl heteroaromatic iodides

Cosimo G. Fortuna *, Vincenza Barresi, Giuseppe Musumarra

Dipartimento di Scienze Chimiche, Università di Catania, Viale A. Doria, 6, 95125 Catania, Italy

ARTICLE INFO

Article history:
Received 10 November 2009
Revised 20 April 2010
Accepted 21 April 2010
Available online 18 May 2010

Dedicated to Prof. Saverio Florio on the occasion of his 70th birthday

Keywords:
Molecular modeling
Antitumor compounds
Heterocycles
QSAR

ABSTRACT

A modeling approach based on physico-chemical and pharmacokinetic properties, called Volsurf+, was used to design new *trans* 2-(thiophen-2-yl)vinyl heteroaromatic iodides with antiproliferative activity. The synthesis and in vitro antitumor tests on two cell lines (MCF-7 and LNCap) confirmed Volsurf predicted activity values. An Almond model, derived to have an overall structural insight on the above compounds, supported the validity of Volsurf and provided guidelines for the synthesis of new compounds.

1. Introduction

Previous work on the design, the synthesis and the antitumor activity of new *trans* 1-heteroaryl-2-(1,3-dimethylimidazolium-2-yl) ethylenes[1] confirmed the hypothesis, based on a Molecular Interaction Field (MIF)[2,3] approach using Grid Independent Descriptors GRIND,[4] that the presence of three aromatic moieties and of halogen atoms are the main structural features necessary to obtain satisfactory antiproliferative activities. The synthesis, QSAR modeling, and biological[5–8] assay of vinyl and halo-furan derivatives has been reported and their activities as antibacterials and anticancer drugs evaluated together with their toxicity effects.[9–12] Recent work of our group on the design of new *trans* 2-(furan-2-yl)vinyl heteroaromatic iodides,[13] using a new chemo-informatic tool, Volsurf+, including both modeling of ADME properties in the design of new structures and the correlation 3D molecular fields with physico-chemical and pharmacokinetic properties, was adopted for predicting the in vitro antitumor activity of these new compounds. In this context we here report the design, the synthesis and the biological evaluation of new *trans* 2-(thiophen-2-yl)vinyl heteroaromatic iodides. In this work, using Volsurf+ and the previously derived model,[13] we design some new structure replacing the O atom of the pentatomic ring with sulfur and predicting their in vitro activities. The structural modifications suggested by the above molecular modeling approach will be verified by the synthesis of the designed molecules and by their activities evaluation tests against two tumor cell lines, MCF-7 and LNCap.

2. Results and discussion

The structures of the new thiophene derivatives are reported in Scheme 1. Eleven structures **4**–**14** previously synthesised and modeled using a program called Almond based on a structural classification were analyzed by the novel methodology called Volsurf+. Volsurf is an automatic procedure to convert 3D molecular fields into physico-chemically relevant molecular descriptors. Volsurf extracts the information present in 3D molecular field maps into few quantitative numerical descriptors, easy to understand and interpret. Molecular recognition is achieved coupling image analysis software with external chemical knowledge. Within this context Volsurf selects molecular descriptors referred to molecular size and shape, to size and shape of both hydrophilic and hydrophobic regions and to the balance between them. Hydrogen bonding, amphiphilic moments, critical packing parameters are other useful descriptors. The Volsurf descriptors have been presented and explained in detail.[13] The originality of Volsurf resides in the fact that surfaces, volumes and other related descriptors can be directly obtained from 3D molecular fields and can be used for multivariate model building to correlate the 3D molecular structures with biological behavior.[14] The Volsurf methodology can also be

* Corresponding author. Tel.: +39 0957385004; fax: +39 095580138.
E-mail address: cg.fortuna@unict.it (C.G. Fortuna).

0968-0896/$ - see front matter © 2010 Elsevier Ltd. All rights reserved.
doi:10.1016/j.bmc.2010.04.060

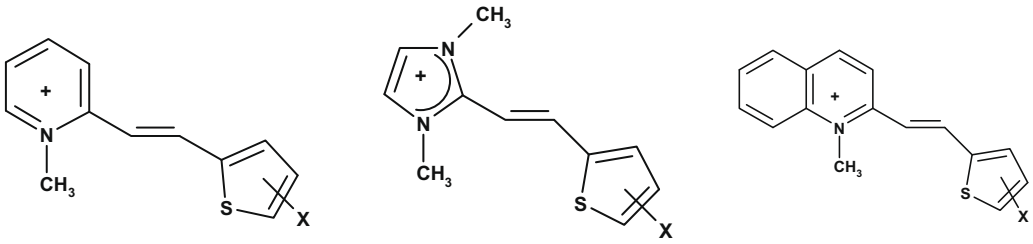

1 2 3

X	Designation
5-Chloro	a
4-Phenyl	b
5-Phenyl	c
5thiophen	d

Scheme 1. Structure of 2-(thiophen-2yl)vinyl-heteroaromatic iodides.

applied for structure–activity relationships and molecular diversity based on surface properties. The test set consist in 11 compounds **4**–**14** reported in Scheme 2, nine of which used to derive the model for furan rings as previously published by our group,[13] plus one thiophene and one *N*-methylpyrrole derivatives; the above compounds exhibited both good and low activities against two tumor cell lines, MCF-7 and LNCap. The best variation of antitumor activity values for these 11 compounds was shown on MCF-7 cell line and we decided, as a consequence, to adopt the MCF-7 values for modeling the structures and predicting the activities of the new compounds. The code number and the antiproliferative in vitro activities for the 11 compounds chosen as test set are reported in Table 1. The 3D structures of these compounds were imported, in Mol-file, and coded as Volsurf descriptors following the procedure described in Section 3.1. Volsurf offer a tool, called Volsurf+ designer, that makes us able to design new compounds and to project them on our test set model. This tool enables to predict the activity of new structures by means of the scores plot projection providing guidelines in the selection of new compounds to be synthesised. Figure 1 reports the 11 structures of the test set and as an example one of the new compounds (**3b**). The background is colored according to the activity values; the red zone indicates higher activity and the yellow point is the new structure. It is possible to note that the predicted activity of **3b** is higher than that of the compounds previously published. In Table 2 the predicted activities for 10 new structures are reported.

This result encouraged to proceed with the synthesis and in vitro biological evaluation of the above derivatives. The synthesis of *trans* 2-(thiophen-2-yl)vinyl heteroaromatic iodides can be easily achieved by condensation of imidazolium, pyridinium or quinolinium iodides with heteroaromatic aldehydes in the presence of NaOH or piperidine (see Section 3), exploiting the acidity of the above salts α methyls due to the electronwithdrawing effect of the adjacent positively charged ring nitrogens.

Under appropriate experimental conditions pure *trans* isomers were obtained, as evidenced by the ethylenic protons *J* coupling constants in the NMR spectra. The antiproliferative activity of all the newly synthesized compounds was then tested against two tumor cell lines, breast carcinoma (MCF-7) and prostate carcinoma (LNCap). The in vitro activities, expressed as log GI_{50} values (see Section 3), are recorded in Table 2. It is worth mentioning that, in order to obtain comparable biological tests, log GI_{50} in Table 2 were all measured in the same experiment. The percent of growth and the inhibition exerted by different doses (0.01–100 μM) are recorded in Figure 2 for MCF-7 cell line and in Figure 3 for LNCap. In addition to antiproliferative effects (log GI_{50}), all the derivatives exhibit a significant cytotoxic activity, expressed as log LC_{50} values as reported in Table 3. Figure 4 reports the experimental activity values for the new structures (yellow points) and for the test set (black points) versus those predicted by the Volsurf model. Experimental values for the designed compounds are similar or even coincident to the predicted ones confirming the potentialities of the Volsurf approach to plan an intelligent selection of new active compounds to be synthesised and tested. In order to verify the validity of Volsurf and to have an overall structural insight an Almond model was also derived for all compounds **1**–**14**.

PLS of ALMOND descriptors relative to compounds **1**–**14** afforded a 5 PC model explaining 99.0% of variance, 73.7% 1st PC, 8.3% 2nd PC, 11.0% 3rd PC, 4.9% 4th PC and 1.0% 5th PC. Figure 5, the scores plot depicting the data structure elucidated by 3 PC (already explaining more than 90% of variance) appears a simplified graphical representation for an immediate evaluation of 3D structural MIF results for compounds **1**–**14** when interacting with the three above mentioned probes. Figure 5 shows that very active compounds such as **7**, **8** and **14**, exhibit a low value in *x* axis, which can reasonably be assumed as a direction representative of antitumor activities. Experimental in vitro values, reported in Table 3 for compounds **1b**, **2c**, **3d** and especially **3b** and **3c** support the overall structural insight provided by the Almond model. Relevant information on the changes in molecular structures in relation to their interactions with the selected Almond probes (Dry, O, and N1) can be obtained by an inspection of the correlograms. In the correlogram for the hydrophobic probe (Fig. 6) compound **8**, the most active of the test set, shows minor interactions with respect to those of the designed structure **3c**, the most active against both tumor cell lines, and to other derivatives containing four aromatic rings. This consideration provides guidelines for the synthesis of new compounds exhibiting increased interactions with probe DRY.

3. Experimental

3.1. Computational methods

3.1.1. Volsurf+ descriptors

The interaction of molecules with biological membranes is mediated by surface properties such as shape, electrostatic forces, H-bonds and hydrophobicity. Therefore, the GRID[15] force field was chosen to characterize potential polar and hydrophobic interaction sites around target molecules by the water (OH_2), the hydrophobic (DRY), and the carbonyl oxygen (O) and amide nitrogen (N1) probe. The information contained in the MIF is transformed into a quantitative scale by calculating the volume or the surface of the

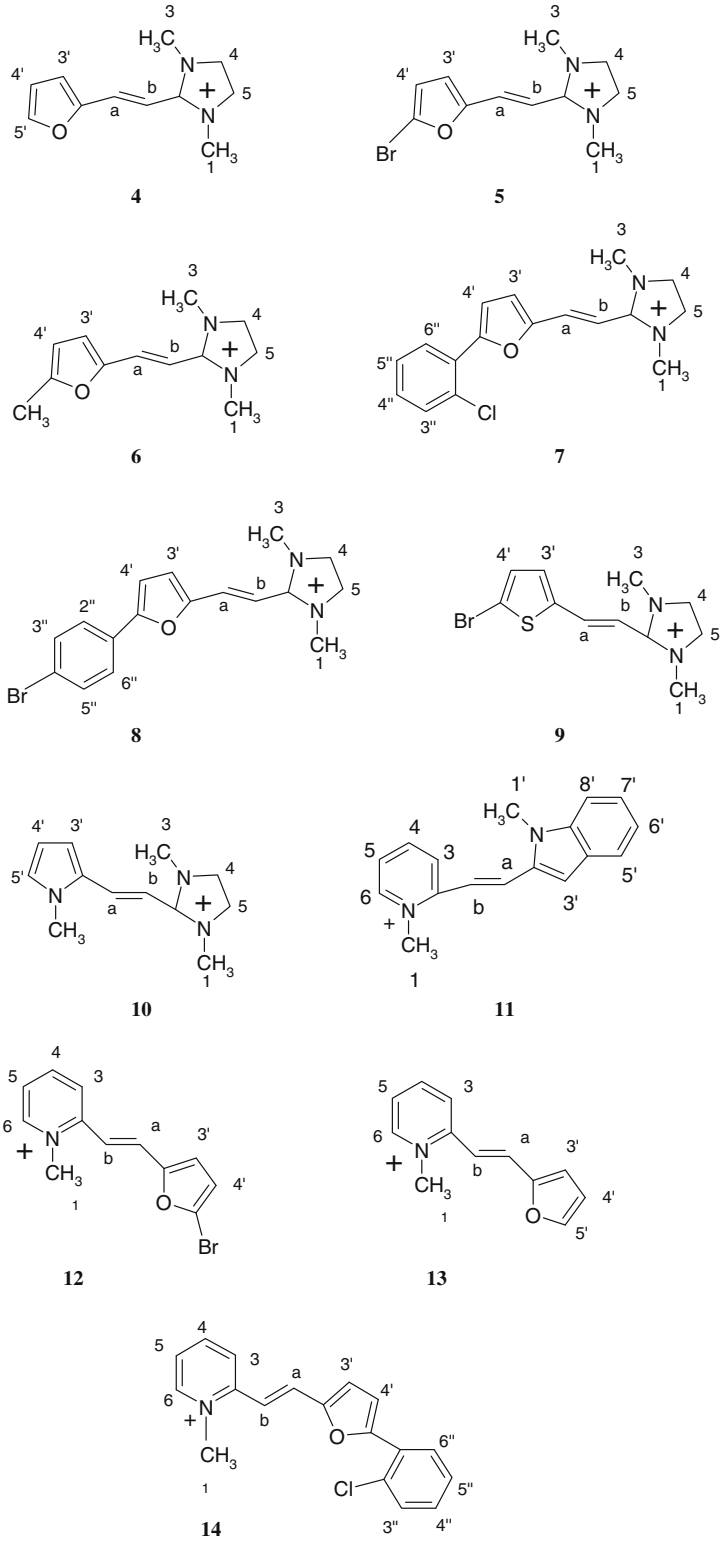

Scheme 2. Structure of compounds for the test set.

interaction contours. The Volsurf+ procedure is as follows: (i) in the first step, the 3D molecular field is generated from the interactions of the OH_2, the DRY, O and N1 probe around a target molecule; (ii) the second step consists in the calculation of descriptors from the 3D maps obtained in the first step. The molecular descriptors obtained, called Volsurf+ descriptors, refer to molecular size and shape, to hydrophilic and hydrophobic regions and to the balance between them, to molecular diffusion, log *P*, log *D*, to the "*charge state*" descriptors, to the new 3D pharmacophoric descriptors and to some descriptors on some relevant ADME properties. The definition of all 126 Volsurf+ descriptors is given in[16–20] (case studies with the old versions of Volsurf) and reported in detail in Table 3; (iii) finally, chemometric tools (PCA,[21] PLS[22]) are used to create relationships of the Volsurf+ descriptor matrix with ADME properties. The scheme of the Volsurf+ programme steps and a detailed definition of Volsurf+ descriptors have recently been reported.[13]

Table 1
Activity values for compounds in the test set against MCF-7 cell line

Compounds	log GI_{50} (μM)
4	−4.00
5	−4.40
6	−4.48
7	−5.86
8	−6.21
9	−4.84
10	−4.00
11	−4.82
12	−5.10
13	−4.15
14	−5.65

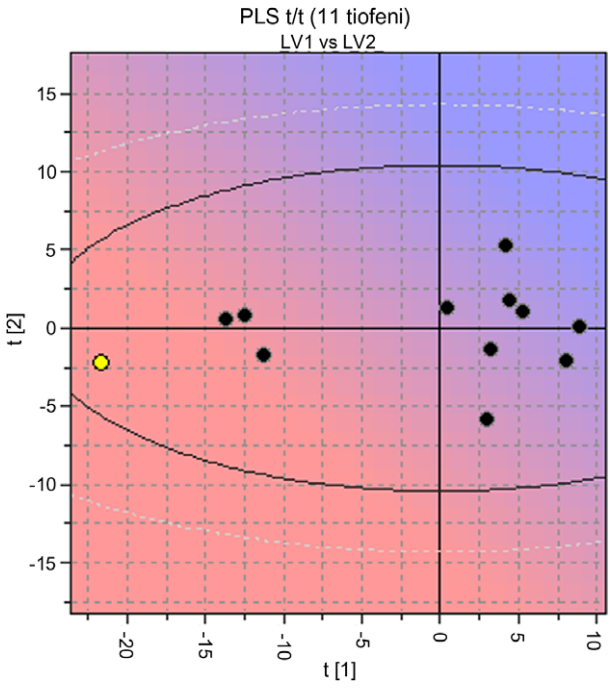

Figure 1. Volsurf scores plot of the test set and of the new structure **3b**.

Table 2
Predicted and in vitro activity values expressed as log GI_{50}, for the designed compounds

Compounds	Predicted activity values	In vitro activity MCF-7	In vitro activity LNCap
3a	−5.68	−5.68	−4.98
1b	−5.84	−6.28	−5.12
2b	−5.62	−6.00	−4.70
3b	−6.59	−6.30	−5.84
1c	−5.67	−5.08	−4.47
2c	−5.50	−5.84	−5.08
3c	−6.36	−6.25	−6.40
1d	−5.67	−5.76	−5.50
2d	−5.81	−5.33	−5.22
3d	−6.52	−5.85	−6.42

3.2. ALMOND

MIF were obtained using the program GRID version 20.[23] GRIND were generated, analyzed, and interpreted using the program ALMOND version 3.0.0 [www.moldiscovery.com] a software package developed in our group. Computations and graphical display were performed on SGI O2 workstations (MIPS R12000 processor). The process of ligand–receptor interaction has often been represented with the help of the MIF.

If a compound is known to bind a certain receptor, some of the regions defined in its Virtual Receptor Site (VRS)[4] should actually overlap groups of the real receptor site and, therefore, at least a subset of the VRS regions would be relevant for representing the binding properties of the ligand. For the latter statement to be true the VRS must have been obtained from the bioactive conformation of the ligand and the probes used to compute it should represent chemical groups present in the binding site. The molecular descriptors presented in this work are based on the concept of VRS. Basically, GRIND are a small set of variables representing the geometrical relationships between relevant regions of the VRS and as such are independent of the coordinate frame of the space where the MIF is computed. The procedure for obtaining GRIND involves three steps: (i) computing a set of MIF, (ii) filtering the MIF to extract the most relevant regions that define the VRS, and (iii) encoding the VRS into the GRIND variables.

3.2.1. Molecular description: GRID Force Field

The GRID program[24–26] was used to describe the molecular structures. GRID is a computational procedure for detecting

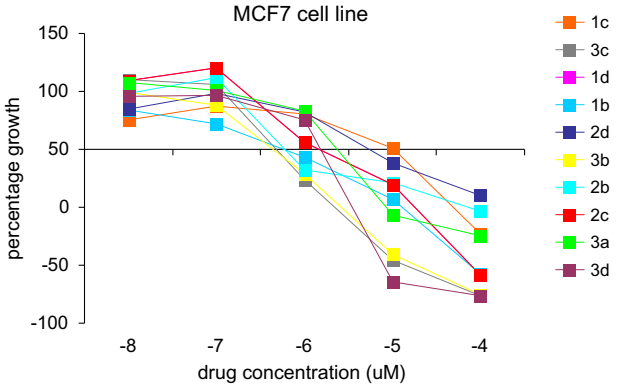

Figure 2. Dose–response curves of antiproliferative activities versus MCF-7.

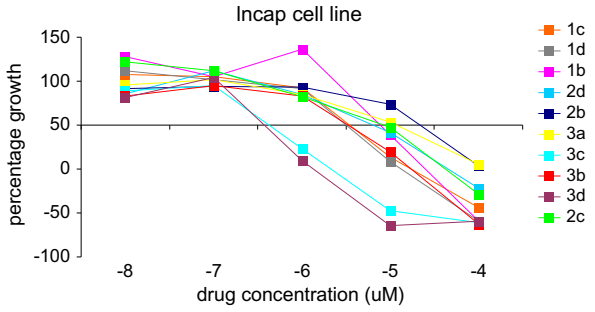

Figure 3. Dose–response curves of antiproliferative activities versus LNCap.

Table 3
In vitro antitumor activities, expressed as log LC_{50}, for MCF-7 and LNCap cell lines

Cell line	Compounds									
	3a	**1b**	**2b**	**3b**	**1c**	**2c**	**3c**	**1d**	**2d**	**3d**
MCF-7	–	−4.11	–	−4.75	–	–	−4.81	−4.11	–	–
LNCap	–	−4.16	–	−4.16	–	–	−4.96	−4.20	–	−5.19

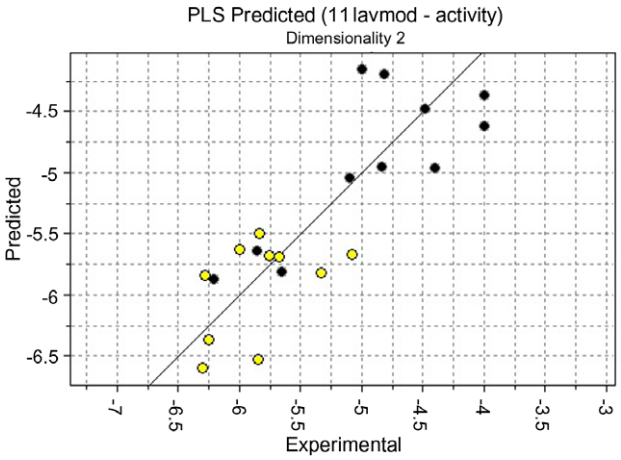

Figure 4. Experimental against Volsurf predicted values for the new structures (yellow) and for the test set (black).

energetically favorable binding sites on molecules. The program calculates the interactions between the molecule and a probe group which is moved through a regular grid of points in a region of interest around the target molecule and, at each point, the interaction energy between the probe and the target molecule is calculated as the sum of Lennard–Jones (E_{LJ}), hydrogen bond (E_{HB})

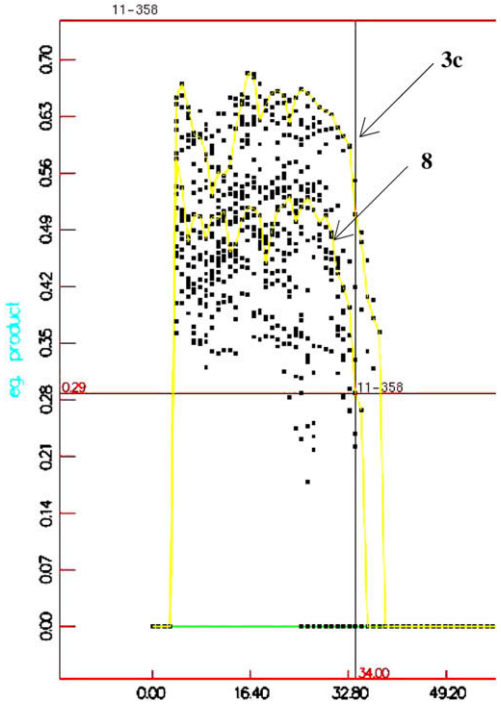

Figure 6. Correlograms for compounds **1**–**14** with the hydrophobic probe.

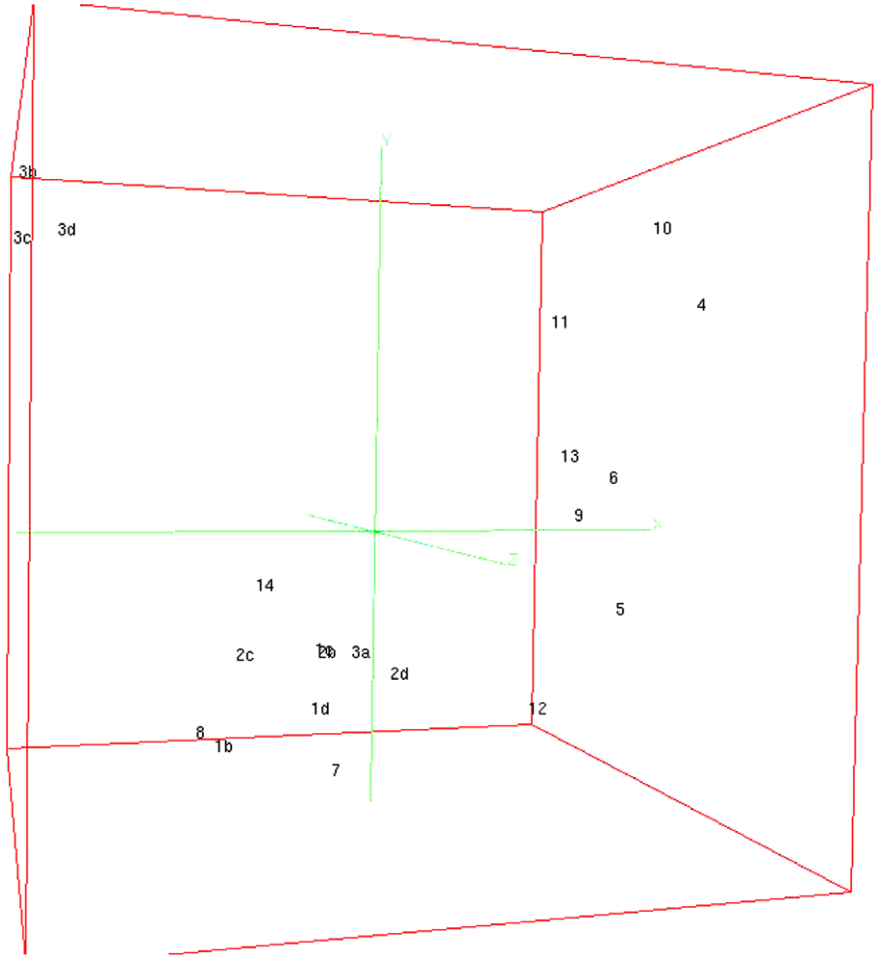

Figure 5. Three components PLS scores plot for Almond descriptors relative to compounds **1**–**14**.

electrostatic interactions (E_{EL}) and, for specific probes, entropic contribution (E_{ENT}):

$$E_{x,y,z} = \sum_{i=1}^{N} E_{LJ} + \sum_{i=1}^{N} E_{HB} + \sum_{i=1}^{N} E_{EL} + \sum_{i=1}^{N} E_{ENT}$$

GRID contains a table of parameters to describe each type of atom occurring in each of the ligand molecules. These parameters define the strength of the Lennard–Jones, hydrogen bond and electrostatic interactions made by an atom and are used in order to evaluate the energy functions. GRID probes are very specific. They give precise spatial information, and this specificity and sensitivity are an advantage since the probes may then be representative of the important chemical groups present in the active site provided that the statistical method used for the analysis can distinguish between different types of interactions.

3.3. Compounds

Heteroaromatic carboxaldehydes were Aldrich commercial products. ^{1}H NMR spectra were recorded on a Varian Unity *Inova* spectrometer operating at 500 MHz, at 25 °C in $(CD_3)_2SO$ using TMS or acetone (2.225 ppm) as internal standards. The spectral width was set to 5000 Hz, with an excitation pulse of 60°, an acquisition time of 3.5 s and a digital resolution after zero-filling of 0.15 Hz/pt. NMR data were processed using MestReC software (http://www.mestrec.com).

Electron Spray Ionization mass spectra were recorded on a Thermo Finnigan LCQ Deca mass spectrometer equipped with a ESI source.

2-Heteroaryl thiophene derivatives, all iodide salts, were obtained by refluxing in ethanol equimolar amounts of 1,2,3-trimethylimidazolium iodide, or 1,2-dimethylpicolinium iodide or 1,2-dimethylquinolinium iodide and the appropriate heteroaromatic aldehyde in the presence of few drops 20% NaOH or piperidine. The resulting precipitate was recrystallized from ethanol.

Details on the synthetic conditions and products characterization are reported below:

3.3.1. 1-Methyl-2-[(*E*)-2-(5-chloro-thiophen-2-yl)-vinyl]-quinolinium iodide (3a)

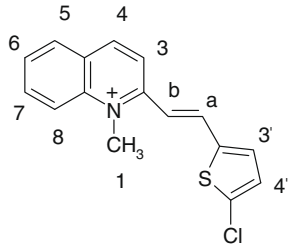

From 1,2-dimethylquinolinium iodide (150 mg, 5.4×10^{-1} mmol) and 5-chloro-2-thiophencarboxaldehyde (56 µl, 5.4×10^{-1} mmol) in 4 ml of refluxing ethanol. The mixture was stirred for 2 h. Red solid (61.81 mg, 2.16×10^{-1} mmol, 40%). Mp 189 °C; ^{1}H NMR (500 MHz, DMSO-d_6, 25 °C): δ = 8.3 (1H, d, J = 16 Hz, H_a), 7.5 (1H, d, J = 15.5 Hz, H_b), 4.48 (3H, s, H_1), 8.31 (1H, d, J = 7 Hz, H_3), 8.56 (1H, d, J = 9 Hz, H_4), 8.44 (1H, d, J = 9 Hz, H_6), 7.93 (1H, t, J = 8 Hz, H_7), 8.17 (1H, t, J = 7 Hz, H_8), 9.01 (1H, d, J = 9 Hz, H_9), 7.14 (1H, d, J = 3.5 Hz, $H_{3'}$), 6.54 (1H, d, J = 3.5 Hz, $H_{4'}$); ESI: m/z 286.2 [M$^+$].

3.3.2. 1-Methyl-2-[(*E*)-2-(4-phenyl-thiophen-2-yl)-vinyl]-pyridinium iodide (1b)

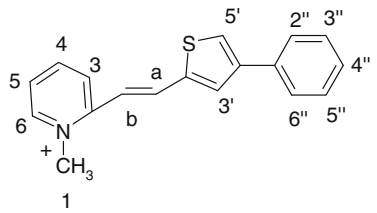

From 1,2-dimethylpyridinium iodide (100 mg, 4.25×10^{-1} mmol) and 4-phenyl-2-thiophencarboxaldehyde (80.1 mg, 4.25×10^{-1} mmol) in 2.5 ml of refluxing ethanol. The mixture was stirred for 4 h. Yellow needles (93 mg, 2.29×10^{-1} mmol, 55%). Mp 202–203 °C; ^{1}H NMR (500 MHz, DMSO-d_6, 25 °C): δ = 8.12 (d, J = 15.5 Hz, 1H, Ha), 7.38 (d, J = 16 Hz, 1H, Hb), 4.35 (s, 3H, CH_3), 8.48 (m, 2H, H_3 e H_4), 7.88 (m, 1H, H_5); 8.88 (d, J = 6.5 Hz, 1H, H_6), 8.17 (s, 1H, $H_{3'}$), 8.15 (d, J = 4.0 Hz, 1H, $H_{5'}$), 7.76 (d, J = 7.5 Hz, 2H, $H_{2''}$ $H_{6''}$), 7.46 (t, J = 7.5 Hz, 2H, $H_{3''}$ e $H_{5''}$), 7.35 (t, J = 7.5 Hz, 1H, $H_{4''}$); ESI: m/z 278.28 [M$^+$].

3.3.3. 1,3-Dimethyl-2-[(*E*)-2-(4-phenyl-thiophen-2-yl)-vinyl]-1*H*-imidazolium iodide (2b)

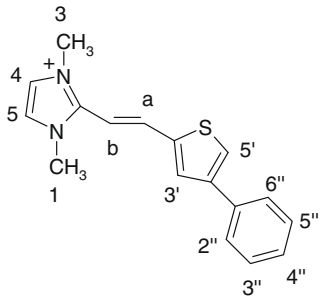

From 1,2,3-trimethylimidazolium iodide (100 mg, 4.20×10^{-1} mmol) and 4-phenyl-2-thiophencarboxaldehyde (79.2 mg, 4.20×10^{-1} mmol) in 2.5 ml of refluxing ethanol. The mixture was stirred for 6 h. Yellow needles (70 mg, 1.72×10^{-1} mmol, 41%). Mp 222–224 °C; ^{1}H NMR (500 MHz, DMSO-d_6, 25 °C): δ = 7.73 (d, J = 16.5 Hz, 1H, H_a), 7.05 (d, J = 16, 5 Hz, 1H, H_b), 3.30 (s, 6H, H_1 e H_3), 7.74 (s, 2H, H_4 e H_5), 8.12 (s, 1H, $H_{3'}$), 8.09 (s, 1H, $H_{5'}$), 7.74 (m 2H, $H_{2''}$ $H_{6''}$), 7.46 (t, J = 8.0 Hz, 2H, $H_{3''}$ e $H_{5''}$), 7.34 (t, J = 7.5 Hz, 1H, $H_{4''}$); ESI: m/z 281.28 [M$^+$].

3.3.4. 1-Methyl-2-[(*E*)-2-(4-phenyl-thiophen-2-yl)-vinyl]-quinolinium iodide (3b)

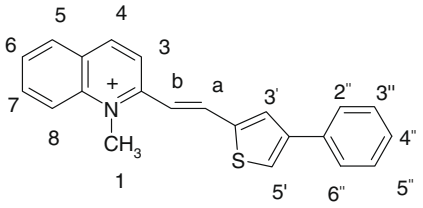

From 1,2-dimethylquinolinium iodide (200 mg, 7.2×10^{-1} mmol) and 4-phenyl-2-thiophencarboxaldehyde (131.7 mg, 7.2×10^{-1} mmol) in 4 ml of refluxing ethanol. The mixture was stirred for 2 h. Brown solid (66.16 mg, 2.016×10^{-1} mmol, 28%). Mp 200 °C; ^{1}H NMR (500 MHz, DMSO-d_6, 25 °C): δ = 8.41 (d, J = 15.5 Hz, 1H, H_a), 7.75 (d, J = 15.5 Hz, 1H, H_b), 4.55 (s, 3H, H_1), 8.34 (d, J = 8 Hz, 1H, H_3), 8.55 (d, J = 9 Hz, 2H, H_4, H_6), 7.95 (t, J = 8 Hz, 1H, H_7), 8.18 (t, J = 8.5 Hz, 1H, H_8), 9.04 (d, J = 9 Hz, 1H, H_5), 8.33 (s, 1H, $H_{5'}$), 8.29 (s, 1H, $H_{3'}$), 7.79 (d, J = 7.5 Hz, 2H, $H_{2''}$, $H_{6''}$), 7.48 (t, J = 7.5 Hz, 2H, $H_{3''}$, $H_{5''}$), 7.37 (t, J = 7.5 Hz, 1H, $H_{4''}$); ESI: m/z 328.2 [M$^+$].

3.3.5. 1-Methyl-2-[(*E*)-2-(5-phenyl-thiophen-2-yl)-vinyl]-pyridinium iodide (1c)

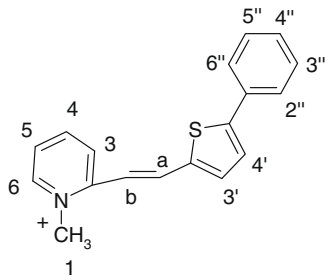

From 1,2-dimethylpyridinium iodide (100 mg, 4.25×10^{-1} mmol) and 5-phenyl-2-thiophencarboxaldehyde (80.1 mg, 4.25×10^{-1} mmol) in 2.5 ml of refluxing ethanol. The mixture was stirred for 8 h. Brown needles (93 mg, 2.29×10^{-1} mmol, 55%). Mp 202–203 °C; ^{1}H NMR (500 MHz, DMSO-d_6, 25 °C): δ = 8.16 (d, J = 15.5 Hz, 1H, Ha), 7.26 (d, J = 16 Hz, 1H, Hb), 3.30 (s, 3H, CH_3), 8.47 (d, 2H, H_3 H_5), 7.86 (dd, 1H, H_4); 8.87 (d, J = 5.5 Hz, 1H, H_6), 6.67 (d, 2H, $H_{3'}$ $H_{4'}$), 8.15 (d, J = 4.0 Hz, 1H, $H_{5'}$), 7.75 (d, J = 8 Hz, 2H, $H_{2''}$ $H_{6''}$), 7.48 (t, J = 7.5 Hz, 2H, $H_{3''}$ e $H_{5''}$), 7.40 (t, J = 7.5 Hz, 1H, $H_{4''}$); ESI: m/z 278.35 [M^+].

3.3.6. 1,3-Dimethyl-2-[(*E*)-2-(5-phenyl-thiophen-2-yl)-vinyl]-1*H*-imidazolium iodide (2c)

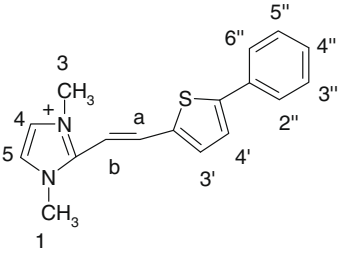

From 1,2,3-trimethylimidazolium iodide (100 mg, 4.20×10^{-1} mmol) and 5-phenyl-2-thiophencarboxaldehyde (79.2 mg, 4.20×10^{-1} mmol) in 2.5 ml of refluxing ethanol. The mixture was stirred in absence of light for 5 h. Yellow needles (76 mg, 1.86×10^{-1} mmol, 44%). Mp 222–224 °C; ^{1}H NMR (500 MHz, DMSO-d_6, 25 °C): δ = 7.74 (d, J = 16.5 Hz, 1H, Ha), 6.94 (d, J = 16.5 Hz, 1H, Hb), 3.30 (s, 6H, H_1 e H_3), 7.73 (s, 2H, H_4 e H_5), 7.63 (d, J = 3.5 Hz, 1H, $H_{3'}$), 7.61 (d, J = 3.5 Hz, 1H, $H_{4'}$), 7.72 (d, J = 6.0 Hz, 2H, $H_{2''}$ $H_{6''}$), 7.47 (t, J = 7.5 Hz, 2H, $H_{3''}$ e $H_{5''}$), 7.38 (t, J = 7.5 Hz, 1H, $H_{4''}$); ESI: m/z 281.35 [M^+].

3.3.7. 1-Methyl-2-[(*E*)-2-(5-phenyl-thiophen-2-yl)-vinyl]-quinolinium iodide (3c)

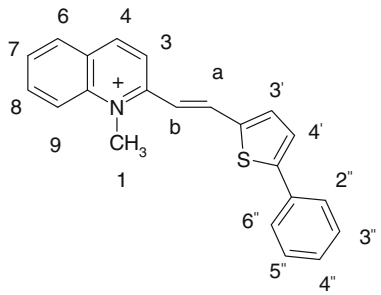

From 1,2-dimethylquinolinium iodide (200 mg, 7.2×10^{-1} mmol) and 5-phenyl-2-thiophencarboxaldehyde (131.7 mg, 7.2×10^{-1} mmol) in 4 ml of refluxing ethanol with one drop of piperidine. The mixture was stirred for 2 h. Dark red solid (67 mg, 2.02×10^{-1} mmol, 30%). Mp 230 °C; ^{1}H NMR (500 MHz, DMSO-d_6, 25 °C): δ = 8.46 (d, J = 15.5 Hz, 1H, H_a), 7.61 (d, J = 15.5 Hz, 1H, H_b), 4.51 (s, 3H, H_1), 8.33 (d, J = 8 Hz, 1H, H_3), 8.53 (d, J = 9 Hz, 1H, H_4), 8.54 (d, J = 9.5 Hz, 1H, H_6), 7.94 (t, J = 7.5 Hz, 1H, H_7), 8.17 (t, J = 7.5 Hz, 1H, H_8), 9.02 (d, J = 9 Hz, 1H, H_5), 7.75 (d, J = 3.5 Hz, 1H, $H_{4'}$), 7.84 (d, J = 3.5 Hz, 1H, $H_{3'}$), 7.79 (d, J = 7.5 Hz, 2H, $H_{2''}$, $H_{6''}$), 7.50 (t, J = 7.5 Hz, 2H, $H_{3''}$, $H_{5''}$), 7.42 (t, J = 7 Hz, 1H, $H_{4''}$); ESI: m/z 328.2 [M^+].

3.3.8. 2-((*E*)-2-[2,2′]Bithiophenyl-5-yl-vinyl)-1-methyl-pyridinium iodide (1d)

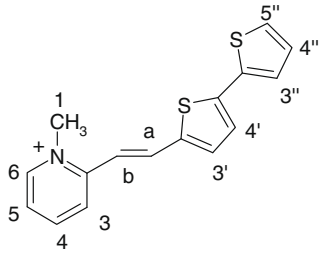

From 1,2-dimethylpyridinium iodide (100 mg, 4.25×10^{-1} mmol) and 2,2′-bithiophen-5-carboxaldehyde (82.4 mg, 4.25×10^{-1} mmol) in 2 ml of refluxing ethanol with two drops of piperidine. The mixture was stirred for 8 h. Red solid (60.1 mg, 1.46×10^{-1} mmol, 34%). Mp 200–202 °C; ^{1}H NMR (500 MHz, DMSO-d_6, 25 °C): δ = 8.14 (d, J = 15.5 Hz, 1H, Ha), 7.21 (d, J = 16 Hz, 1H, Hb), 4.34 (s, 3H, CH_3), 8.45 (m, 2H, H_3 H_5), 7.84 (m, 1H, H_4); 8.86 (d, J = 6 Hz, 1H, H_6), 7.64 (d, J = 4.5 Hz, 1H, $H_{3'}$), 7.60 (d, J = 4.0 Hz, 1H, $H_{4'}$), 7.45 (d, J = 4 Hz, 1H, $H_{5''}$), 7.48 (d, J = 3.5 Hz, 1H, $H_{3''}$), 7.07 (t, J = 4.0 Hz, 1H, $H_{4''}$); ESI: m/z 284.2 [M^+].

3.3.9. 2-((*E*)-2-[2,2′]Bithiophenyl-5-yl-vinyl)-1,3-dimethyl-1*H*-imidazolium iodide (2d)

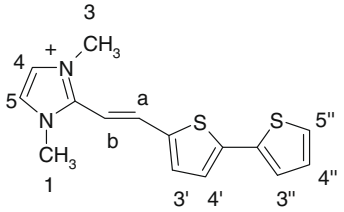

From 1,2,3-trimethylimidazolium iodide (100 mg, 4.20×10^{-1} mmol) and 2,2′-bithiophen-5-carboxaldehyde (81.5 mg, 4.20×10^{-1} mmol) in 3 ml of refluxing ethanol. The mixture was stirred in absence of light for 7 h. Brown solid (84 mg, 2.03×10^{-1} mmol, 48%). Mp 215–217 °C; ^{1}H NMR (500 MHz, DMSO-d_6, 25 °C): δ = 7.742 (d, J = 16.5 Hz, 1H, Ha), 6.91 (d, J = 16.5 Hz, 1H, Hb), 3.74 (s, 6H, H_1 e H_3), 7.62 (s, 2H, H_4 e H_5), 7.54 (d, J = 4 Hz, 1H, $H_{3'}$), 7.41 (d, J = 3.5 Hz, 1H, $H_{4'}$), 7.61 (dd, J = 5.0 Hz, 1H, $H_{3''}$), 7.15 (dd, J = 5.0 Hz, 1H, $H_{4''}$), 7.45 (dd, J = 3.5 Hz, 1H, $H_{5''}$); ESI: m/z 287.24 [M^+].

3.3.10. 2-((*E*)-2-[2,2′]Bithiophenyl-5-yl-vinyl)-1-methyl-quinolinium iodide (3d)

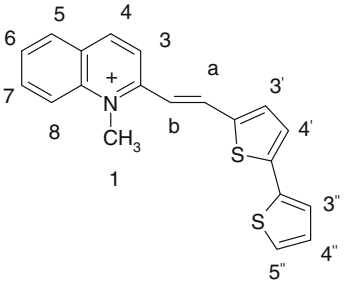

From 1,2-dimethylquinolinium iodide (200 mg, 7.2×10^{-1} mmol) and 2,2′-bithiophen-5-carboxaldehyde (135.9 mg, 7.2×10^{-1} mmol) in 4 ml of refluxing ethanol with one drop of piperidine. The mixture

was stirred for 7 h. Dark solid (153 mg, 4.6×10^{-1} mmol, 67%). Mp 229 °C; ^{1}H NMR (500 MHz, DMSO-d_6, 25 °C): δ = 8.43 (d, J = 15.5 Hz, 1H, H_a), 7.57 (d, J = 15.5 Hz, 1H, H_b), 4.50 (s, 3H, H_1), 8.332 (d, J = 8 Hz, 1H, H_3), 8.52 (d, J = 9 Hz, 1H, H_4), 8.53 (d, J = 9 Hz, 1H, H_6), 7.93 (t, J = 7.5 Hz, 1H, H_7), 8.16 (t, J = 7 Hz, 1H, H_8), 9 (d, J = 9 Hz, 1H, H_5), 7.77 (d, J = 4 Hz, 1H, $H_{3'}$), 7.68 (d, J = 5 Hz, 1H, $H_{3''}$), 7.53 (d, J = 3.5 Hz, 1H, $H_{4'}$), 7.54 (d, J = 4.5 Hz, 1H, $H_{5''}$), 7.18 (t, J = 5 Hz, 1H, $H_{4''}$); ESI: m/z 334 [M^+].

4. Biological essays

4.1. Human cell lines (MCF-7 and LNCap)

Human prostate adenocarcinoma cells (LNCap) were grown in RPMI 1640. Human mammary adenocarcinoma (MCF-7) were grown in Dulbecco's MEM (DMEM), 1.0 g/L D-glucose. Each medium was supplemented with 10% (v/v) heat-inactivated fetal bovine serum, 2 mM L-alanyl-L-glutamine, penicillin–streptomycin (50 U–50 μg for ml) and incubated at 37 °C in humidified atmosphere of 5% CO_2, 95% air. The culture medium was changed twice a week.

4.2. Treatment with antitumor agents and MTT colorimetric assay

Human cancer cell line (5×103 cells/0.33 cm^2) was plated in 96-well plates "Nunclon TM Microwell TM" (Nunc) and were incubated at 37 °C. After 24 h, cells were treated with the compounds (final concentration 0.01–100 μM). Untreated cells were used as controls. Microplates were incubated at 37 °C in humidified atmosphere of 5% CO_2, 95% air for 3 days and then cytotoxicity was measured with colorimetric assay based on the use of tetrazolium salt MTT (3-(4,5-dimethylthiazol-2-yl)-2,5-diphenyl tetrazolium bromide).[27] The results were read on a multiwell scanning spectrophotometer (Multiscan reader), using a wavelength of 570 nm. Each value was the average of 8 wells (standard deviations were less than 20%). The GI_{50} value was calculated according to NCI: thus, GI_{50} is the concentration of test compound where $100 \times (T - T0)/(C - T0) = 50$ (T is the optical density of the test well after a 48-h period of exposure to test drug; $T0$ is the optical density at time zero; C is the control optical density).

Acknowledgment

We thank the University of Catania for financial support.

References and notes

1. Ballistreri, F. P.; Barresi, V.; Benedetti, P.; Caltabiano, G.; Fortuna, C. G.; Longo, M. L.; Musumarra, G. *Bioorg. Med. Chem.* **2004**, *12*, 1689.
2. Goodford, P. *J. Med. Chem.* **1985**, *28*, 849.
3. Cramer, R. D., III; Patterson, D. E.; Bunce, J. *J. Am. Chem. Soc.* **1988**, *110*, 5959.
4. Pastor, M.; Cruciani, G.; McLay, I.; Pickett, S.; Clementi, S. *J. Med. Chem.* **2000**, *43*, 3233.
5. González-Díaz, H.; Agüero, G.; Cabrera, M. A.; Molina, R.; Santana, L.; Uriarte, E.; Delogu, G.; Castañedo, N. *Bioorg. Med. Chem. Lett.* **2005**, *15*, 551.
6. González-Diaz, H.; Marrero, Y.; Hernandez, I.; Bastida, I.; Tenorio, E.; Nasco, O.; Uriarte, E.; Castanedo, N.; Cabrera, M. A.; Aguila, E.; Marrero, O.; Morales, A.; Perez, M. *Chem. Res. Toxicol.* **2003**, *16*, 1318.
7. González-Díaz, H.; Cruz-Monteagudo, M.; Molina, R.; Tenorio, E.; Uriarte, E. *Bioorg. Med. Chem.* **2005**, *13*, 1119.
8. Estrada, E. *Mutat. Res.* **1998**, *420*, 67.
9. González-Díaz, H.; Olazábal, E.; Santana, L.; Uriarte, E.; González-Díaz, Y.; Castañedo, N. *Bioorg. Med. Chem.* **2007**, *15*, 962.
10. González-Díaz, H.; Torres-Gómez, L. A.; Guevara, Y.; Almeida, M. S.; Molina, R.; Castañedo, N.; Santana, L.; Uriarte, E. *J. Mol. Model.* **2005**, *11*, 116.
11. González-Díaz, H.; Tenorio, E.; Castañedo, N.; Santana, L.; Uriarte, E. *Bioorg. Med. Chem.* **2005**, *13*, 1523.
12. González Borroto, J. I.; Pérez Machado, G.; Creus, A.; Marcos, R. *Mutagenesis* **2005**, *20*, 193.
13. Fortuna, C. G.; Barresi, V.; Berellini, G.; Musumarra, G. *Bioorg. Med. Chem.* **2008**, *16*, 4150.
14. Doddareddy, M. R.; Cha, J. H.; Cho, Y. S.; Koh, H. Y.; Yoo, K. H.; Kim, D. J.; Pae, A. N. *Bioorg. Med. Chem.* **2005**, *13*, 3339.
15. Carosati, E.; Sciabola, S.; Cruciani, G. J. *J. Med. Chem.* **2004**, *47*, 5114.
16. Cruciani, G.; Crivori, P.; Carrupt, P. A.; Testa, B. *J. Mol. Struct.* **2000**, *503*, 17.
17. Crivori, P.; Cruciani, G.; Carrupt, P. A.; Testa, B. *J. Med. Chem.* **2000**, *43*, 2204.
18. Cruciani, G.; Meniconi, M.; Carosati, E.; Zamora, I.; Mannhold, R.. In *Methods and Principles in Medicinal Chemistry*; van de Waterbeemd, H., Lennernäs, H., Artursson, P., Eds.; Wiley-VCH, 2003; Vol. 18, p 406.
19. Berellini, G.; Cruciani, G.; Mannhold, R. *J. Med. Chem.* **2005**, *48*, 4389.
20. Mannhold, R.; Berellini, G.; Carosati, E.; Benedetti, P.. In *Molecular Interaction Fields*; Cruciani, G., Mannhold, R., Kubinyi, H., Folkers, G., Eds.; Wiley-VCH Verlag GmbH & Co. KGaA: Weinheim, 2006; Vol. 27, p 173.
21. Wold, S.; Sjöström, M. In *Chemometrics: Theory and Application*, Kowalski, B. R., Eds.; ACS Symposium Series, Washington, 1977; pp 243.
22. Wold, S.; Albano, C.; Dunn, W. J., III; Edlund, U.; Esbensen, K.; Geladi, P.; Hellberg, S.; Johansson, E.; Lindberg, W.; Sjöström, M. In *Chemometrics*, Kowalski, B. R., Ed., 1984; pp 17.
23. GRID v. 20 Molecular Discovery Ltd.
24. Goodford, P. J. *J. Med. Chem.* **1985**, *28*, 849.
25. Boobbyer, D. N. A.; Goodford, P. J.; Mcwhinnie, P. M.; Wade, R. C. *J. Med. Chem.* **1989**, *32*, 1083.
26. Wade, R.; Clerk, K. J.; Goodford, P. J. *J. Med. Chem.* **1993**, *36*, 140.
27. Mosmann, T. J. *J. Immunol. Methods* **1983**, *65*, 55.